JBC RESEARCH ARTICLE

An allosteric redox switch in domain V of β_2-glycoprotein I controls membrane binding and anti-domain I autoantibody recognition

Received for publication, April 10, 2021, and in revised form, June 9, 2021 Published, Papers in Press, June 29, 2021,
https://doi.org/10.1016/j.jbc.2021.100890

Suresh Kumar[1,‡], **Mathivanan Chinnaraj**[1,‡], **William Planer**[1], **Xiaobing Zuo**[2], **Paolo Macor**[3], **Francesco Tedesco**[4], **and Nicola Pozzi**[1,*]

From the [1]*Edward A. Doisy Department of Biochemistry and Molecular Biology, Saint Louis University School of Medicine, St Louis, Missouri, USA;* [2]*X-Ray Science Division, Argonne National Laboratory, Lemont, Illinois, USA;* [3]*Department of Life Sciences, University of Trieste, Italy; and* [4]*Istituto Auxologico Italiano, IRCCS, Laboratory of Immuno-Rheumatology, Milan, Italy*

Edited by Joseph Jez

β_2-glycoprotein I (β_2GPI) is an abundant multidomain plasma protein that plays various roles in the clotting and complement cascades. It is also the main target of antiphospholipid antibodies (aPL) in the acquired coagulopathy known as antiphospholipid syndrome (APS). Previous studies have shown that β_2GPI adopts two interconvertible biochemical conformations, oxidized and reduced, depending on the integrity of the disulfide bonds. However, the precise contribution of the disulfide bonds to β_2GPI structure and function is unknown. Here, we substituted cysteine residues with serine to investigate how the disulfide bonds C32-C60 in domain I (DI) and C288-C326 in domain V (DV) regulate β_2GPI's structure and function. Results of our biophysical and biochemical studies support the hypothesis that the C32-C60 disulfide bond plays a structural role, whereas the disulfide bond C288-C326 is allosteric. We demonstrate that absence of the C288-C326 bond, unlike absence of the C32-C60 bond, diminishes membrane binding without affecting the thermodynamic stability and overall structure of the protein, which remains elongated in solution. We also document that, while absence of the C32-C60 bond directly impairs recognition of β_2GPI by pathogenic anti-DI antibodies, absence of the C288-C326 disulfide bond is sufficient to abolish complex formation in the presence of anionic phospholipids. We conclude that the disulfide bond C288-C326 operates as a molecular switch capable of regulating β_2GPI's physiological functions in a redox-dependent manner. We propose that in APS patients with anti-DI antibodies, selective rupture of the C288-C326 disulfide bond may be a valid strategy to lower the pathogenic potential of aPL.

β_2-glycoprotein I (β_2GPI), also known as apolipoprotein H, is a phospholipid-binding protein that plays multiple roles in the coagulation and complement cascades (1–4). It is also recognized as the main antigen of antiphospholipid antibody (aPL) in the autoimmune disorder antiphospholipid syndrome (APS) (1). β_2GPI consists of 326 amino acids organized in four canonical complement control protein (CCP) domains (DI-DIV) (5, 6) followed by an aberrant CCP-like domain, DV, which is held responsible for the interaction with a variety of negatively charged surfaces, such as heparin and "activated" plasma membranes (7–10). Other important structural features of β_2GPI are four N-glycosylations, which account for ~20% of its molecular weight (11), and 22 conserved cysteines (C), potentially forming 11 disulfide bonds (Fig. 1*A*).

Even though there is some disagreement regarding the structural architecture of the protein while it circulates in the blood (8–10, 12–14), consensus exists on the fact that, in human plasma, β_2GPI adopts two major interconvertible redox states, oxidized (54%) and reduced (46%), depending on the disulfide bonds' integrity (15, 16). In the oxidized form, all 22 cysteine residues are oxidized, forming 11 disulfide bonds (S-S). By contrast, in the reduced form, some of the 11 disulfide bonds are broken. While the exact number of oxidized and reduced species present in human plasma has yet to be defined, pioneering studies led by the group of Krilis have revealed that oxidized β_2GPI is the substrate of several thiol-isomerases and can be reduced by this family of enzymes both *in vitro* and *in vivo* (17), in which case the disulfide bond most heavily targeted is C288-C326 in DV, followed by C32-C60 in DI (18).

While the mechanisms controlling the redox equilibrium of β_2GPI have yet to be fully understood, similar to other plasma proteins (see Table 1 in Chiu and Hogg (19)), oxidation/reduction cycles may provide a means of regulation of its biological function, with important consequences in APS (20, 21) and other cardiovascular diseases in which patients are subjected to higher levels of oxidative stress (22). For instance, while the oxidized form of β_2GPI was shown to inhibit platelet adhesion to immobilized von Willebrand Factor (vWF) under flow conditions (23), the reduced form was shown to increase adhesion of platelet *via* platelet glycoprotein Ib alpha (GpIbα) (18). Another functional difference between oxidized and reduced β_2GPI is that reduced β_2GPI protected cells of the vasculature from free radical injury, perhaps working as a chemical scavenger (16, 24). Finally, it was also documented that the levels of oxidized β_2GPI were significantly elevated in

‡ These authors contributed equally to this work.
* For correspondence: Nicola Pozzi, nicola.pozzi@health.slu.edu.

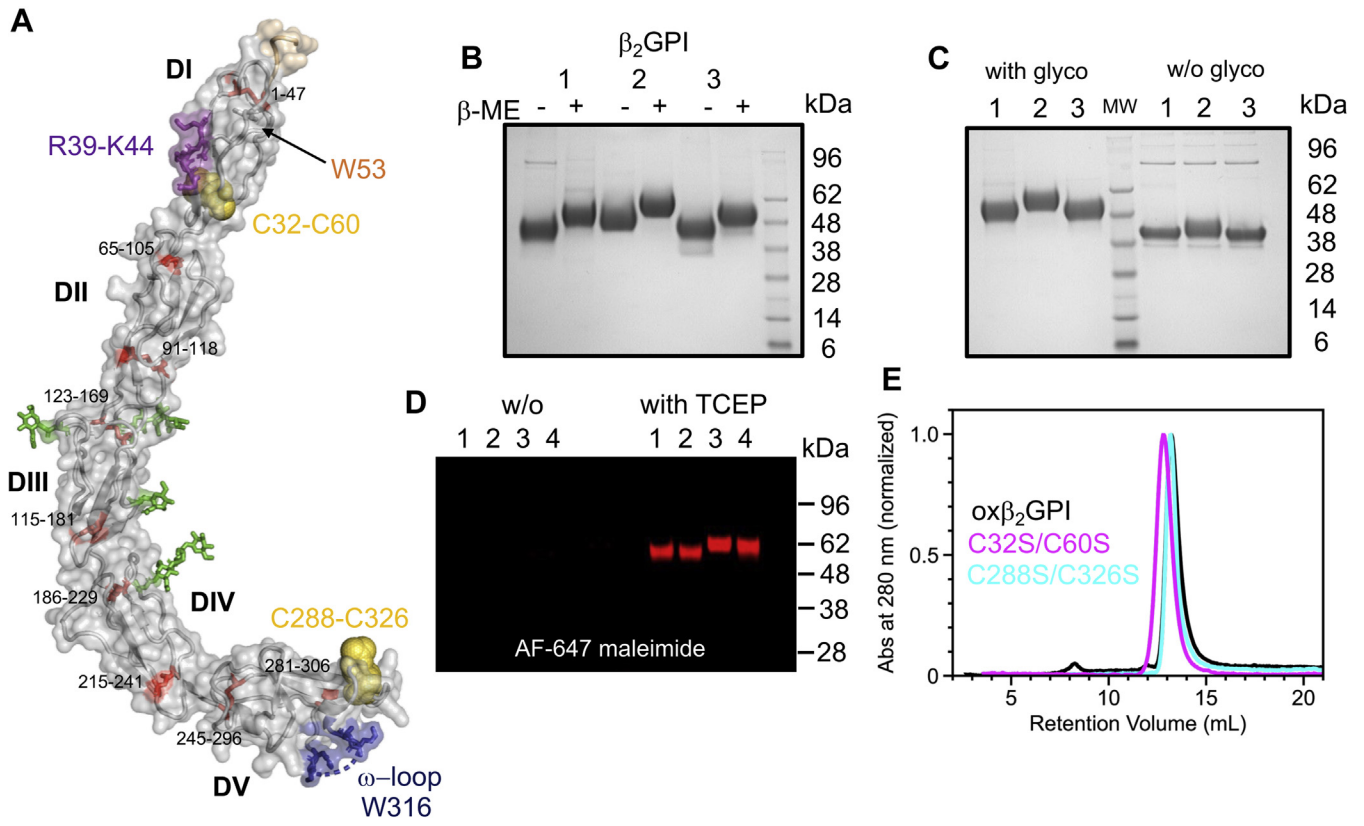

Figure 1. Chemical characterization and oligomeric state of the reduced-like variants. *A*, X-ray crystal structure of oxβ$_2$GPI (6V09) (10) documenting integrity of the 11 disulfide bonds (*red sticks*) and the location of the two disulfide bonds in DI targeted in this study (*yellow spheres*). Also highlighted are other regions of the molecules relevant for this study: the N-terminal HPC4 tag (*wheat*); the epitope R39-K44, which is recognized by MBB2 (10); residue W53 in DI (*orange*), the ω-loop (311–317), and W316 in DV, which is not visible in the structure due to disorder. Glycosylations are shown as green sticks. *B*, SDS-PAGE analysis of the recombinant proteins before (–) and after (+) the treatment with the reducing agent β-mercaptoethanol (β-ME). Samples are 1 = oxβ$_2$GPI; 2 = β$_2$GPI C32S/C60S; 3 = β$_2$GPI C288S/C326S. *C*, SDS-PAGE analysis of the recombinant proteins before (*left*) and after (*right*) removal of the glycosylations. Samples are 1 = oxβ$_2$GPI; 2 = β$_2$GPI C32S/C60S; 3 = β$_2$GPI C288S/C326S. Note how the deglycosylation treatment reduce the difference of electrophoretic mobility between the samples, indicating that β$_2$GPI C32S/C60S contains more glycans when produced in HEK293 cells. *D*, reactivity of the recombinant proteins against AF-647 maleimide in the absence (*left*) and presence (*right*) of TCEP monitored by SDS-PAGE. Samples are 1 = oxβ$_2$GPI; 2 = β$_2$GPI C288S/C326S; 3 and 4 = β$_2$GPI C32S/C60S. Bands 3 and 4 are two different preparations of β$_2$GPI C32S/C60S, which document minimal lot-to-lot variability. *E*, shown are the chromatograms obtained by SEC documenting monomeric proteins and a slightly but appreciable difference between the variant β$_2$GPI C32S/C60S and the other two samples. The small shift is in agreement with the larger hydrodynamic radius documented by SDS-PAGE in *panels B–D*.

APS patients with an active form of the disease (25), raising the hypothesis that oxidized β$_2$GPI is the preferred target of aPL. In contrast to this hypothesis, studies published by Buchholz *et al.* (13) while completing this manuscript documented a strong increase in the binding of aPL to reduced β$_2$GPI that was prepared by thioredoxin reduction followed by 3-(N-maleimido-propionyl) biocytin (MPB) labeling to avoid reoxidation. Hence, it remains unclear under what circumstances aPL prefers oxidized or reduced β$_2$GPI.

Based on this premise and encouraged by our previous structural analyses of human recombinant β$_2$GPI (10), we set out to investigate the structural and functional consequences imparted by the selective rupture of the disulfide bonds C32-C60 in DI and C288-C326 in DV of β$_2$GPI. Differently from previous studies, in which chemical or enzymatic methods were used to reduce disulfide bonds of β$_2$GPI (13, 17, 26), chemically stable, reduced-like forms of β$_2$GPI were produced using genetic methods by replacing cysteine residues with serine. The C→S replacement makes the formation of disulfide bonds impossible. At the same time, given that serine differs from cysteine in a single atom—the oxygen of the alcohol replaces the sulfur of the thiol—serine substitutions are likely to preserve the H-bonding network imparted by the thiol groups, which is lost when thiols are reacted with chemicals such as MPB. Hence, replacement of C→S at positions 32 and 60 in DI and 288 and 326 in DV should provide a reasonable experimental model to study the effects caused by the rupture of each disulfide bond.

Results

Removal of C32-C60 and C288-C326 disulfide bonds in β$_2$GPI does not affect protein expression levels and oligomeric state

The double mutants β$_2$GPI C32S/C60S and β$_2$GPI C288S/C326S were expressed in human embryonic kidney cells alongside β$_2$GPI WT (Fig. 1*A*). Because β$_2$GPI WT contains 22 cysteines forming 11 disulfide bonds (10), in this study, we named it oxidized β$_2$GPI (oxβ$_2$GPI). Purification of the proteins from the media was performed by immunoaffinity

chromatography under mild buffer conditions (20 mM Tris pH 7.4, 145 mM NaCl, TBS) by taking advantage of a calcium-dependent tag located at the N-terminus (10). This strategy was chosen to preserve the structural and chemical integrity of the recombinant proteins. Yields of ~0.5 mg per liter of cell culture were obtained for all three proteins, documenting similar expression levels.

Immunopurified proteins migrated as a single smeary band at ~50 kDa under nonreducing and reducing conditions, indicative of a single, heavily glycosylated polypeptide chain (Fig. 1*B*). Interestingly, the band of β_2GPI C32S/C60S displayed a slightly lower electrophoretic mobility compared with oxβ_2GPI, implying a larger hydrodynamic radius. Since no such difference was observed for β_2GPI C288S/C326S, we attributed this effect to a higher content of glycosylations, which may have resulted from a partial disruption of the DI's secondary structure. In line with this interpretation, the difference between β_2GPI C32S/C60S and oxβ_2GPI almost completely disappeared after 3 h of deglycosylation treatment (Fig. 1*C*). Thus, unlike C→S substitutions at positions 288 and 326 in DV, substitutions at positions 32 and 60 in DI enhanced glycan incorporation during protein synthesis, possibly as a result of local structural perturbations in DI.

In addition to introducing local structural perturbations, absence of the disulfide bond in DI may result in global disulfide bond instability. This was investigated by reacting β_2GPI C32S/C60S with AlexaFluor-647-C2-maleimide in the absence and presence of the reducing agent tris(2-carboxyethyl)phosphine hydrochloride (TCEP), as performed recently with protein disulfide isomerase (27). oxβ_2GPI and β_2GPI C288S/C326S were used as a control. Regardless of the protein sample, incorporation of the fluorescent dyes was observed almost exclusively in the presence of TCEP (Fig. 1*D*). This indicates that, in the absence of TCEP, the cysteine residues are incapable of reacting with the maleimide dye, suggesting that they are either oxidized, likely forming chemically stable disulfide bonds, or simply inaccessible to the fluorescent dye, in which case they should be buried, an observation that is consistent with a folded protein structure.

Finally, to elucidate the oligomeric state under native conditions, we performed analytical size-exclusion chromatography (SEC) experiments in 20 mM Tris pH 7.4, 145 mM NaCl, 5 mM $CaCl_2$. The proteins were prepared at 20 μM, resulting in a concentration ~2–4 μM in the column due to dilution. This is the concentration of β_2GPI in human plasma (1). The vast majority (>95%) of β_2GPI C32S/C60S and β_2GPI C288S/C326S eluted in single peaks with retention volumes of ~12.9 ml and ~13.2 ml, respectively (Fig. 1*E*). Importantly, the chromatographic profiles and elution volumes were similar to those obtained for oxβ_2GPI (~13.2 ml). This is consistent with monomeric proteins.

Structural consequences imparted by the loss of the disulfide bonds

We have recently demonstrated that oxβ_2GPI adopts an elongated conformation under physiological pH (*i.e.*, 7.4) and ionic strength concentrations (*i.e.*, 145 mM NaCl) (10). However, the structures of the reduced form(s) of β_2GPI remain unknown. Recent atomic force microcopy (AFM) analyses of reduced β_2GPI produced by enzymatic reaction indicate that reduced β_2GPI absorbed into mica sheets mostly retains a closed form (65%), with a slight preference for the open form when compared with untreated β_2GPI (35% *versus* 25%) (13). However, SEC analysis of the proteins in Figure 1*E* indicates that β_2GPI C32S/C60S and β_2GPI C288S/C326S are similar to oxβ_2GPI and, therefore, should too be elongated in solution. To validate our observations, we performed small-angle X-ray scattering (SAXS) experiments. The scattering profiles and pair distribution functions of the three proteins in TBS buffer are shown in Figure 2*A* and Figure 2*B*, respectively. Data were collected in the presence of ~0.5% (w/w) glycerol, which minimizes radiation damage while preserving proteins' native conformations. From these plots, we calculated radius of gyration (R_g) and maximum linear dimensions (D_{max}) values, which are shown in Figure 2*C*. The values of R_g and D_{max} are similar for oxβ_2GPI and β_2GPI C288S/C326S. These values are consistent with our previously published data for β_2GPI, but not with what AFM analyses would have predicted (13), documenting elongated conformations of oxβ_2GPI and β_2GPI C288S/C326S in solution. Also consistent with the conclusions derived from the SEC experiments in Figure 1*E* are the SAXS data obtained with the mutant β_2GPI C32S/C60S. In this case, the values of R_g and D_{max} were slightly larger than that of oxβ_2GPI (Fig. 2*C*), documenting a more extended conformation of the protein in solution, hence a larger hydrodynamic radius. This difference between the variants is best appreciated in Figure 2*D*, which shows the *ab initio* envelopes calculated from the scattering profiles shown in Figure 2*A*.

Impact of the disulfide bonds on the stability of β_2GPI

Having established that all three proteins are monomeric and adopt elongated structures in solution, we next investigated their thermodynamic stability by chemical denaturation methods. This is because rupture of disulfide bonds often leads to destabilization of a protein's three-dimensional structure, which, in turn, results in different protein denaturation profiles (28). β_2GPI contains five tryptophan residues, one in every domain. Addition of 7M Gnd-HCl to solutions of oxβ_2GPI, β_2GPI C32S/C60S, and β_2GPI C288S/C326S in TBS buffer produced a significant threefold increase of the intrinsic fluorescence signal (Fig. 3*A*). This indicates that (1) in TBS buffer, the proteins are folded, and (2) a high concentration of Gnd-HCl causes the proteins to unfold. These spectroscopic signatures are reminiscent of previous data obtained using chemically synthesized DI (29). They are also consistent with the structure of human recombinant β_2GPI shown in Figure 1*A*. In this structure, residues W53 in DI, W111 in DII, W175 in DIII, and W235 in DIV are buried within the protein core, located in the proximity of a disulfide bond. In contrast, W316 in DV is located in the ω-loop, which is flexible and constitutively exposed to the solvent. Since disulfide bonds

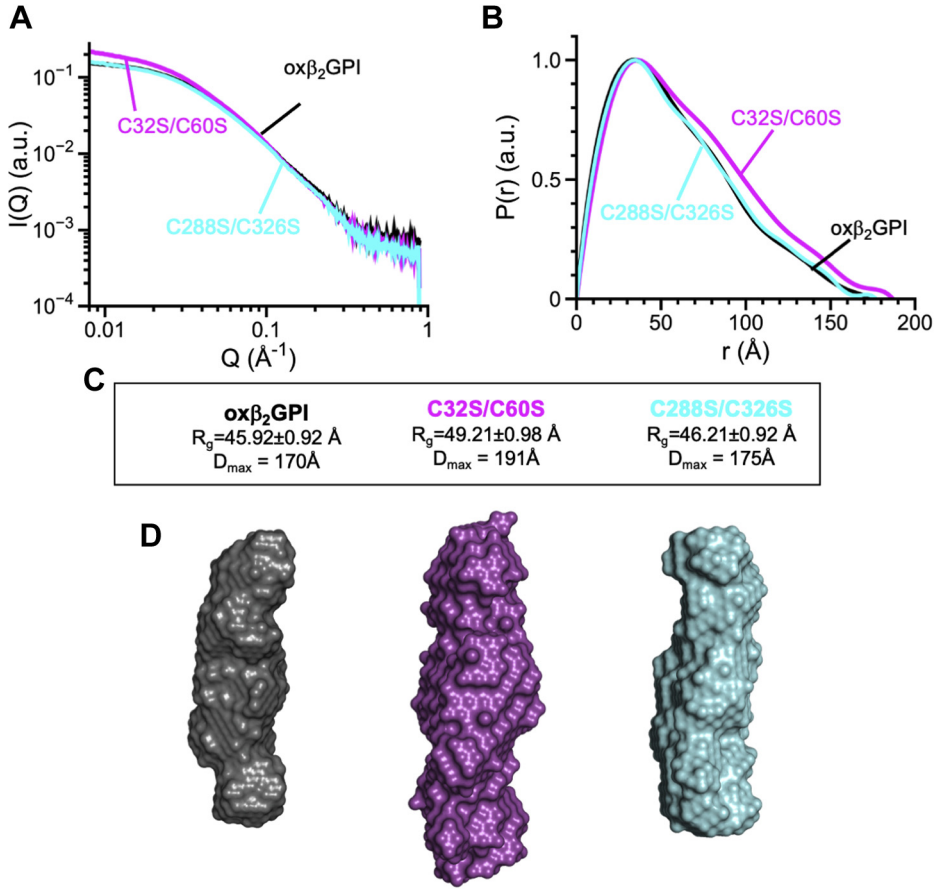

Figure 2. Solution structure of the disulfide bond variants monitored by SAXS. Scattering profiles (*A*) and normalized pair distribution functions (*B*) of oxβ_2GPI (*black*), β_2GPI C32S/C60S (*magenta*), and β_2GPI C288S/C326S (*cyan*) obtained in 20 mM Tris pH 7.4, 145 mM NaCl, 0.5% glycerol (w/w) at a concentration of 4 mg/ml. *C*, radius of gyration (R_g) determined by linear fit from the Guinier plot and D_{max} calculated for each protein sample. *D*, surface representation of the *ab initio* envelopes calculated from the scattering profiles shown in *panel A*. Note how β_2GPI C32S/C60S is significantly more elongated than oxβ_2GPI and β_2GPI C288S/C326S.

quench tryptophan fluorescence by an electron transfer mechanism (30), unfolding of β_2GPI is expected to liberate the tryptophans in DI-DIV, resulting in an increase of the fluorescence signal. In line with this interpretation, we found that the fluorescence intensity of the 280-nm emission spectrum of β_2GPI C32S/C60S was ~35% higher than that of oxβ_2GPI, whereas it did not change for the mutant β_2GPI C288S/C326S. We speculate that, while the chemical environment of W316 is not perturbed by the mutations C288S/C326S, absence of the disulfide bond C32-C60 results in loss of fluorescence

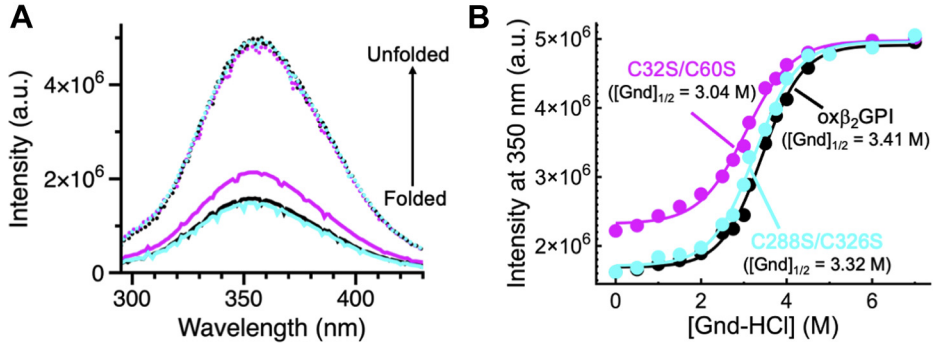

Figure 3. Stability of the disulfide bond variants. *A*, baseline subtracted fluorescence spectra of oxβ_2GPI (*black*), β_2GPI C32S/C60S (*magenta*), and β_2GPI C288S/C326S (*cyan*) (1.0 ml, 0.2 mM in 20 mM Tris pH 7.4, 145 mM NaCl, 0.015% Tween 20 at 25 °C) in the absence (*solid lines*) and presence (*dotted lines*) of 7M Gnd-HCl. *B*, chemical denaturation induced by Gdn-HCl. Protein samples were excited at 280 nm, and the fluorescence intensity was recorded at 350 nm as a function of denaturant concentration. Continuous line represents the best fit of data points to Equation 25 in Eftink (60), yielding a $GdnHCl_{1/2}$ and denaturation index (m) values of 3.41 ± 0.10 M and 0.0140 ± 0.0009 for oxβ_2GPI (*black*), 3.04 ± 0.10 M and 0.0123 ± 0.0010 for β_2GPI C32S/C60S (*magenta*), and 3.32 ± 0.12 M and 0.0132 ± 0.0009 for β_2GPI C288S/C326S (*cyan*). Note how the sigmoidal curves for oxβ_2GPI and β_2GPI C288S/C326S are almost identical but different from β_2GPI C32S/C60S.

quenching, also facilitated by relaxation of the protein secondary structure.

By taking advantage of the denaturant-dependent increase of fluorescence intensity reported in Figure 3*A*, concentration-dependent experiments were performed to quantify the impact of the two disulfide bonds on the stability of β_2GPI (Fig. 3*B*). Sigmoidal curves were obtained for all the constructs, indicative of a cooperative transition between folded and unfolded species (28). Analysis of the fluorescent data with a two-state model (F->U) (29) yielded Gdn-$HCl_{1/2}$ values of 3.41 ± 0.10 M for oxβ_2GPI, 3.04 ± 0.10 M for β_2GPI C32S/C60S, and 3.31 ± 0.12 M for β_2GPI C288S/C326S. While the values of Gdn-$HCl_{1/2}$ were within experimental error for β_2GPI C288S/C326S and oxβ_2GPI, they were significantly different (0.37 units) from those calculated for the variant β_2GPI C32S/C60S. This documents that, unlike C288-C326, the disulfide bond C32-C60 in DI is important for the thermodynamic stability of β_2GPI: its absence facilitates protein unfolding.

A redox switch in DV controls β_2GPI binding to the membranes

An important physiological role of β_2GPI is to clear necrotic and bacteria cells from the circulation and neutralize cell debris (1), such as polyanions, which may cause cellular damage, inflammation, and may trigger coagulation. To evaluate the functional consequences caused by the loss of the disulfide bonds, binding studies were performed using unfractionated heparin and liposomes made of phosphatidylcholine: cardiolipin (POPC:CL, 80:20% molar ratio) and phosphatidylcholine: phosphatidylserine (POPC:POPS, 80:20% molar ratio), as simplified models for necrotic cells, which are also relevant to the role β_2GPI in APS (31, 32).

Chromatographic studies were used to study the interaction of β_2GPI with heparin. This methodology, although qualitative, has been successfully used in the past and proved useful to identify some of the regions responsible for this interaction (33). Consistent with previous reports (33), oxβ_2GPI bound with moderate strength to the heparin column. It eluted from the column at a value of conductivity equals 29 mS/cm, which corresponds to ∼300 mM NaCl (Fig. 4*A*). Likewise, elution of β_2GPI C32S/C60S from the heparin column occurred at 28 mS/cm, documenting no perturbation caused by the mutations in DI. More interesting, however, was the effect of the substitutions C288S/C326S. β_2GPI C288S/C326S bound to heparin better than oxβ_2GPI (28 mS/cm *versus* 33 mS/cm), suggesting that an intact C288-C326 disulfide bond lowers the affinity for heparin.

Next, surface plasmon resonance (SPR) studies were performed to monitor the kinetics of interaction between β_2GPI and immobilized large unilamellar vesicles (LUV) prepared by extrusion. SPR was chosen for two reasons. First, it allows determination of apparent binding affinity constants (K_d), which provide a quantitative description of the system. Second, it provides information about the maximal binding stoichiometry (34), expressed as the number of protein molecules bound at saturation to the outer region of a 100-nm liposome. The sensograms of oxβ_2GPI, β_2GPI C32S/C60S, and β_2GPI C288S/C326S obtained by flowing increasing concentrations of proteins in 20 mM Tris pH 7.4, 145 mM NaCl, 0.1% BSA (w/v) onto a L1 sensor chips immobilized with POPC:CL and POPC:POPS are shown in Figure 4, *B* and *C*, respectively. Maximum response obtained at 50 s plotted *versus* total ligand concentration is shown in Figure 4, *D* and *E* The SPR profiles of oxβ_2GPI and β_2GPI C32S/C60S were qualitatively similar to each other and so were the values of K_d and maximal binding stoichiometry (Fig. 4*F*). In contrast, binding of β_2GPI C288S/C326S to liposomes was reduced compared with oxβ_2GPI. We measured values of $K_{d,app}$ ∼13 and ∼8 times weaker compared with oxβ_2GPI and a maximum binding stoichiometry of 174 and 66 for POPC:CL and POPC:POPS, respectively. This corresponds to one protein-binding site per ∼50 CL and ∼130 POPS, as compared with one protein-binding site per ∼15 CL and ∼35 POPS for oxβ_2GPI and ∼16 CL and ∼38 POPS for β_2GPI C32S/C60S. The remarkable drop in number of β_2GPI molecules bound at saturation for β_2GPI C288S/C326S translates into less protein bound per square nanometer (nm^2). These results are consistent with a model in which the integrity of the disulfide bond C288-C326 in DV regulates binding and accumulation of β_2GPI onto negatively charged plasma membranes.

Binding of pathogenic anti-DI antibodies to β_2GPI is reduced by loss of the disulfide bond C32-C60

Antibodies against β_2GPI (anti-β_2GPI) are considered a hallmark of APS and are believed to play a key role in the disease pathogenesis (35). Among them, the ones targeting DI are considered highly pathogenic (36, 37). We, therefore, evaluated how the mutations C32S/C60S and C288S/C326S might affect anti-β_2GPI recognition. We performed a series of ELISA assays in which β_2GPI was immobilized onto a hydrophilic plastic plate and patients' plasma was used as a source of autoantibodies. Plasma samples from 18 APS patients with lupus anticoagulant (LA) and also positive for anticardiolipin (aCL) and anti-β_2GPI antibodies, so called "triple positive," were chosen for these studies. This is because, in these patients, most anti-β_2GPI antibodies are believed to target DI (38). The results of the ELISA assays are shown in Figure 5*A*. They document that anti-β_2GPI from triple-positive APS patients, while reacting equally well against immobilized oxβ_2GPI and β_2GPI C288S/C326S, reacted very poorly toward immobilized β_2GPI C32S/C60S. Since the difference between oxβ_2GPI and β_2GPI C288S/C326S was not statistically significant ($p > 0.05$), we concluded that loss of the disulfide bond C32-C60, but not C288-C326, impairs autoantibody recognition toward immobilized β_2GPI.

A possible explanation for the data in Figure 5*A*, which is consistent with the biophysical structural studies in Figure 3, is that loss of the disulfide bond C32-C60 results in partial unfolding of DI. This, in turn, may alter the conformation of the loop G40-R43, which is considered the immunodominant epitope of anti-DI antibodies (39). Since patients' autoantibodies are heterogenous, we tested this hypothesis by

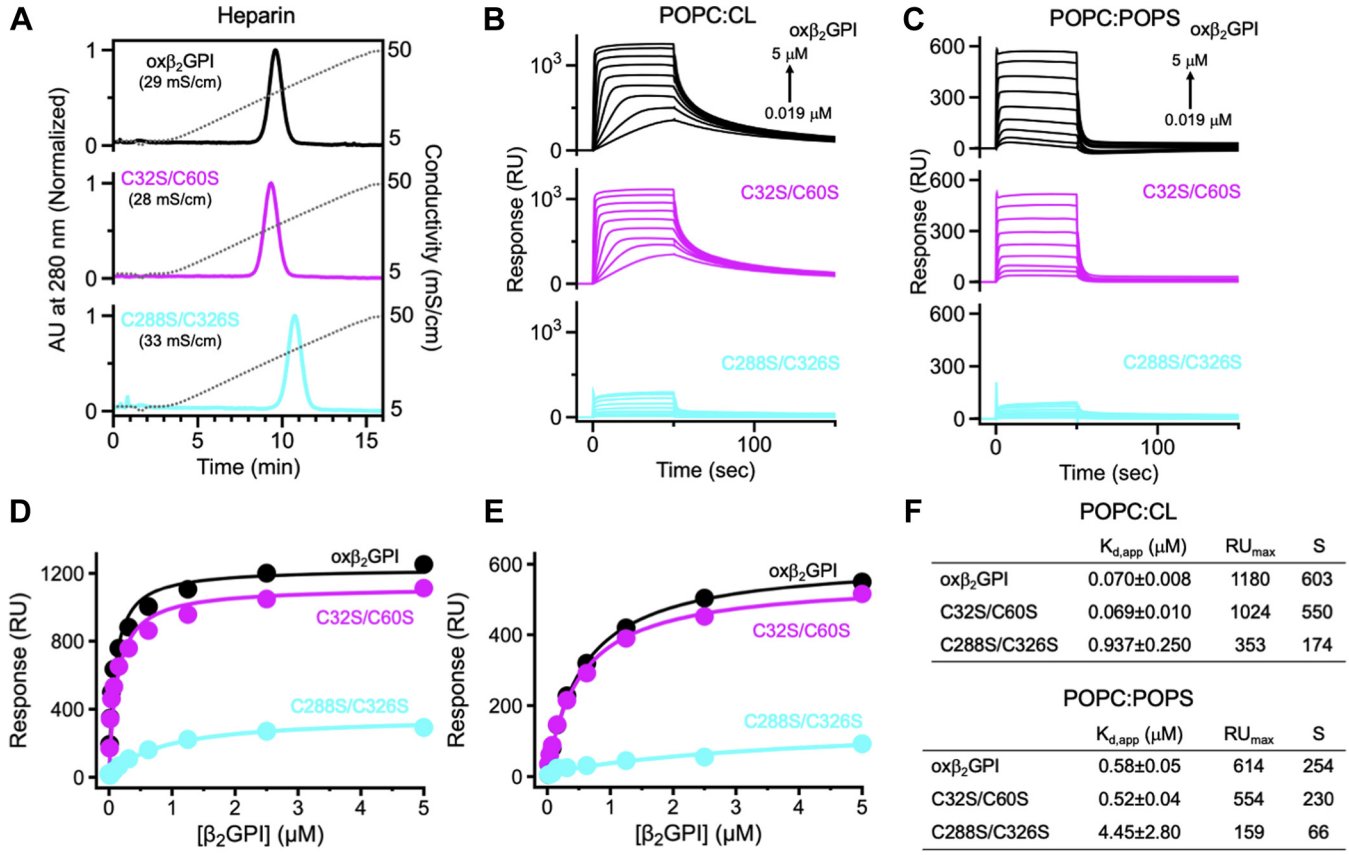

F

POPC:CL

	$K_{d,app}$ (μM)	RU_{max}	S
oxβ2GPI	0.070±0.008	1180	603
C32S/C60S	0.069±0.010	1024	550
C288S/C326S	0.937±0.250	353	174

POPC:POPS

	$K_{d,app}$ (μM)	RU_{max}	S
oxβ2GPI	0.58±0.05	614	254
C32S/C60S	0.52±0.04	554	230
C288S/C326S	4.45±2.80	159	66

Figure 4. Interaction with heparin and plasma membranes. *A*, heparin chromatographic analyses. Samples solubilized in 20 mM Tris pH 7.4 50 mM NaCl were loaded onto a 1 ml HiTrap Heparin column and eluted with a linear gradient of NaCl, from 50 to 500 mM in 15 min (*dotted line*). Flow rate was set to 0.8 ml/min and absorbance was set to 280 nm. Note how the peak center of β_2GPI C288S/C326S (*cyan*) shifts toward the right compared with oxβ_2GPI (*black*) and β_2GPI C32S/C60S (*magenta*), documenting higher affinity for heparin. *B* and *C*, sensograms obtained by injecting increasing concentrations of protein solutions (from 0.019 to 5 μM) into an L1 chip coated with liposomes made of (*B*) POPC:CL (80:20%, 100 nm) and (*C*) POPC:POPS (80:20%, 100 nm). Flow rate was 25 ml/min. Experimental conditions are 20 mM Tris pH 7.4, 145 mM NaCl, 0.1% (w/v) BSA (*D* and *E*) RU values at equilibrium plotted *versus* concentration of β_2GPI (*dots*) and fit to a simple binding isotherm (*line*) to extract values of apparent K_d and RU_{max} reported in *panel F*. Note how oxβ_2GPI (*black*) and β_2GPI C32S/C60S (*magenta*) are similar to each other but different from the variant with the mutations C288S/C326S. *F*, values of affinity, RU_{max}, and stoichiometry (S) calculated by SPR. S was calculated using the formula (RU_protein/RU_liposomes)*(MW_liposome/MW_protein) as described elsewhere (34) and assuming that 50% of the total number of lipids are accessible to the protein.

performing binding studies using the monoclonal antibody MBB2. Previous biochemical studies have shown that MBB2 recognizes the epitope R39-K44 in DI (10) and is pathogenic *in vivo* (40). To allow direct comparison, binding studies were conducted by ELISA, using the same protocol developed for the experiments shown in Figure 5*A*. We found that soluble MBB2 reacted very strongly toward immobilized oxβ_2GPI and β_2GPI C288S/C326S, reaching saturation at a concentration of 1 μg/ml, which corresponds to a molar concentration of 12.5 nM (Fig. 5*B*). By contrast, soluble MBB2 reacted very poorly toward immobilized β_2GPI C32S/C60S, indicating impaired binding. Global fitting of the dose-dependent curves using a Hill equation was used to quantify the differences between the variants. This method yielded EC_{50} values of 0.92 ± 0.1 nM for oxβ_2GPI, 146 ± 20 nM for β_2GPI C32S/C60S, and 0.77 ± 0.1 nM for β_2GPI C288S/C326S, documenting a drop ∼150-fold when the disulfide bond C32-C60 in DI is broken.

Although unlikely due to the conservative nature of the C→S substitutions, the loss of affinity of MBB2 for β_2GPI C32S/C60S may arise from unfolding and/or a preferential orientation upon the interaction with the protein to the plastic surface, resulting in masking of the epitope R39-K44, which is recognized by MBB2. To rule out these possibilities and, at the same time, eliminate the complexity introduced by multiple washing/binding steps associated with ELISA, we performed SPR experiments. MBB2 was immobilized to the chip's surface and β_2GPI was kept in the fluid phase. In agreement with our previously published studies (10), we found that oxβ_2GPI interacted with MBB2 with a K_d = 5.3 ± 0.3 μM (Fig. 5*C*, top panel), characterized by fast association and dissociation rate constants. As for the disulfide bond variants, we found that the binding profile of β_2GPI C288S/C326S was identical to oxβ_2GPI (Fig. 5*C*, bottom panel). In contrast, the binding of β_2GPI C32S/C60S to immobilized MBB2 was approximately 5-fold reduced compared with oxβ_2GPI. Loss of binding was clearly visible by inspecting the sensograms shown in Figure 5*C*, middle panel, and the dose-dependent plots are displayed in Figure 5*D*. This data is qualitatively consistent with the results obtained by ELISA and supports a model whereby anti-β_2GPI antibodies in triple-positive APS patients target an epitope in DI, which is compromised, yet not

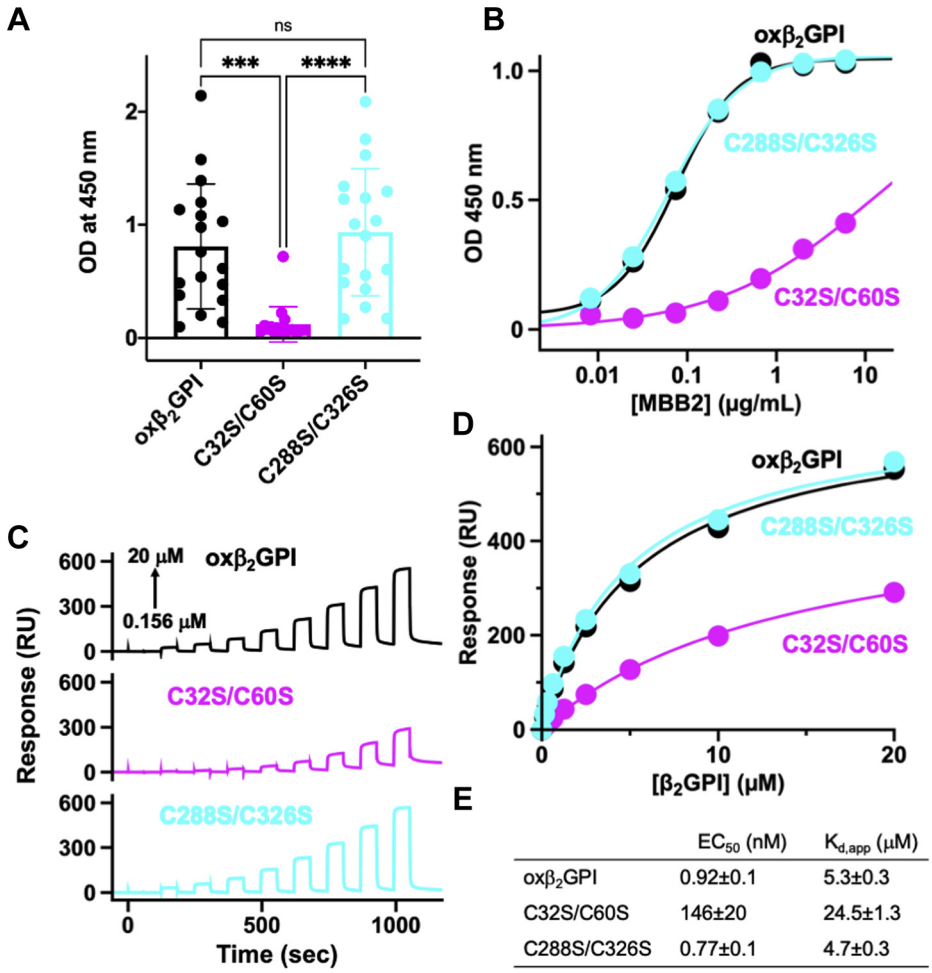

	EC_{50} (nM)	$K_{d,app}$ (μM)
oxβ2GPI	0.92±0.1	5.3±0.3
C32S/C60S	146±20	24.5±1.3
C288S/C326S	0.77±0.1	4.7±0.3

Figure 5. Interaction of β_2GPI with antiphospholipid antibodies. *A*, reactivity of aPL from 18 triple-positive APS patients monitored by ELISA. *Each dot* represents a patient, and the value of each dot is the average of two independent determinations. Statistical analysis between the three groups was performed using ANOVA (*** $p < 0.001$, **** $p < 0.0001$). *B*, binding of MBB2 to immobilized oxβ_2GPI and variants followed by ELISA, using the same protocol for *panel A*. Dose-dependent curves were globally fit to a Hill equation. Best-fit values of EC_{50} are reported in *panel E*. *C*, interaction between immobilized MBB2 and soluble β_2GPI followed by SPR. *D*, maximum response at each concertation was plotted against total concentration of soluble β_2GPI. Dose-dependent curves were globally fit to a simple binding equation. Best-fit values of K_d are reported in *panel E*. Reproducibility was tested by performing each binding experiment two times, by randomizing the order of the injections and immobilizing the same antibody in the two different flow channels. *E*, values of affinity calculated by ELISA (EC_{50}) and SPR ($K_{d,app}$).

disrupted, when the disulfide bond C32-C60 is broken. Differences between the values of affinities measured by ELISA and SPR for MBB2 were expected from previous studies (10, 40), implying that immobilization of the antigen onto the plastic plate results in optimal antigen recognition. Whether conformational changes are responsible for this phenomenon is certainly a possibility. However, such conformational changes must be different from opening of the structure caused by the interaction of circular β_2GPI with the plastic plate inferred by previous studies (12, 13, 37) since the recombinant proteins used in this study are already elongated.

Interplay between disulfide bonds and anti-β_2GPI/β_2GPI complex formation in the presence of anionic phospholipids

Even though our binding assays in Figure 5 document that autoantibodies bind to DI and therefore are not directly affected by the structural integrity of the disulfide bond C288-C326, *in vivo*, pathogenic anti-β_2GPI/β_2GPI complexes often form on the surface of activated or dying cells exposing negatively charged phospholipids and very rarely in solution (40, 41). We, therefore, set out to elucidate the interplay between the integrity of the disulfide bonds and anti-β_2GPI/β_2GPI complex formation in the presence of anionic phospholipids. Similar experiments were recently performed by our group to uncover functional differences between type I and type II antiphosphatidylserine/prothrombin antibodies (aPS/PT) in APS patients (42). To mimic a physiologically relevant scenario, we incubated a fixed concentration of β_2GPI (*i.e.*, 2 μM, the concentration of β_2GPI in human plasma) with increasing concentrations of MBB2 (from 0.01 to 2 μM) in 20 mM Tris pH 7.4, 145 mM NaCl, 5 mM $CaCl_2$, and 0.1% BSA (w/v) and then injected this mixture into a surface coated with POPC:CL. The concentrations of MBB2 were chosen according to previous literature to cover a reasonable range of anti-β_2GPI concentrations found in APS patients (43). Figure 6*A* shows the sensograms obtained for the three protein samples injected into the same phospholipid surface. The

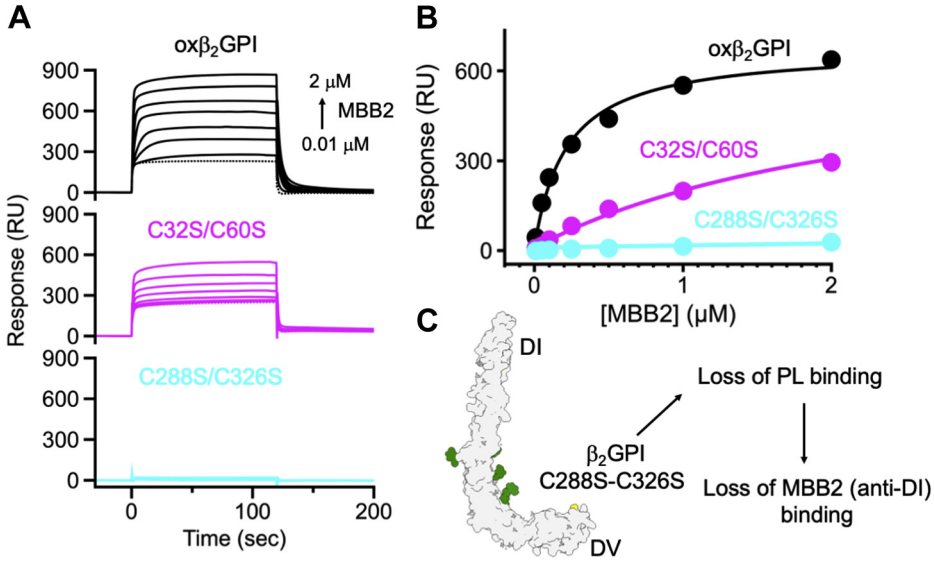

Figure 6. Interplay between anti-DI antibodies and phospholipid binding. *A*, sensograms of oxβ_2GPI and mutants obtained by injecting 2 μM of protein alone (*dotted line*) or protein that was complexed with increasing concentrations of MBB2 (from 0.01 to 2 μM) into an L1 chip coated with POPC:CL (80:20). Flow rate was 25 μl/min. Running buffer was 20 mM Tris pH 7.4, 145 mM NaCl, 5 mM $CaCl_2$, 0.1% (w/v) BSA. *B*, shown is the response at each concentration of MBB2 obtained after 110 s subtracted for the protein alone sample *versus* the concentration of MBB2. *Solid lines* were obtained used the phenomenological equation $y = (R_0 + R_{max}*(x/EC_{50}))/(1+(x/EC_{50}))$ to measure the concentration of MBB2, which provides 50% of the maximum effect (R_{max} = 675 units). *C*, schematic model summarizing the interplay between oxidative modifications, phospholipid binding, and MBB2 binding.

sensograms are interpreted as accumulation of β_2GPI onto the lipids that is amplified by the presence of MBB2. In the presence of MBB2, we observed maximum response for oxβ_2GPI, followed by β_2GPI C32S/C60S. A weak response was measured for β_2GPI C288S/C326S even at the highest concentration of MBB2 tested, which produces saturation of the signal for oxβ_2GPI. Since MBB2 does not bind to the phospholipids, this data provides evidence that multimerization of oxβ_2GPI and β_2GPI C32S/C60S onto the membranes is stimulated by MBB2. It also shows that binding of β_2GPI C288S/C326S to the membranes cannot be rescued by addition of MBB2.

A nonlinear fit of the response *versus* the concentration of MBB2, shown in Figure 6*B*, was used to quantify the difference between the protein samples. This analysis yielded values of EC_{50}, interpreted as the concentration of MBB2, which provides 50% of the maximum effect, of ∼0.2 μM for oxβ_2GPI, ∼2 μM for β_2GPI C32S/C60S, and >90 μM for β_2GPI C288S/C326S, underscoring the remarkable difference between oxβ_2GPI and β_2GPI C288S/C326S and documenting that the presence of anionic phospholipids enhances MBB2 binding of ∼100-fold for oxβ_2GPI. Of note, accumulation of β_2GPI-MBB2 complexes started at concentrations of MBB2 that were significantly lower (>100-fold) than the values of K_d calculated for the proteins in solution, implying that binding of β_2GPI to the lipids precedes antibody binding and that formation of a soluble complex is not necessary to explain the kinetics of binding. Hence, we conclude that oxidized β_2GPI bound to anionic membrane is the preferred target of MBB2 and perhaps other anti-DI antibodies.

Discussion

In this work, we performed biophysical and biochemical studies to characterize how loss of the disulfide bonds C32-C60 and C288-C326 in the plasma glycoprotein β_2GPI perturbs some of its physiological functions, which are also important for aPL binding. Our results lend support to the hypothesis that the disulfide bond C288-C326 acts as a redox switch that regulates membrane binding and, therefore, indirectly controls the formation of immune complexes under conditions most relevant to APS pathology (Fig. 6*C*). Furthermore, we surprisingly found that loss of the disulfide bond C288-C326 stimulates heparin binding (Fig. 4*A*). Since (auto)activation of coagulation factor XII is accelerated by heparin (44, 45), enhanced binding of reduced β_2GPI to polyanions such as heparin, and perhaps polyphosphates (46), could help explain its mild anticoagulant activity in the bloodstream (47). Based on this evidence, mechanisms to preserve the reduced form of β_2GPI in the circulation or stimulate the reduction of the disulfide bond C288-C326 may find utility in the treatment of APS patients. In addition to highlighting the functional role of the disulfide bond C288-C326, our results are also informative because (1) they consolidate previous observations regarding the epitope specificity of anti-β_2GPI antibodies in triple-positive APS patients, who carry the greatest risk of developing thrombosis (10, 38, 39, 48); and (2) they stress the importance of oxidative posttranslational modifications as a highly relevant biological mechanism to fine-tune the function of extracellular proteins involved in hemostasis (49–54).

Differently from previous studies (13, 17, 26), which relied on chemical and enzymatic reduction of disulfide bonds, we generated two variants in which the cysteine residues 32 and 60 in DI and 288 and 326 in DV were substituted to serine. β_2GPI WT, which represents the oxidized monomeric form of β_2GPI (10), was used as a control. We opted for this protein engineering strategy because it overcomes many challenges

associated with the production, purification, and storage of reduced protein species generated by chemical and enzymatic reactions without, however, introducing significant chemical perturbations to the system.

An initial finding documented by SEC (Fig. 1*E*) and SAXS (Fig. 2) made possible by this strategy was that the absence of either disulfide bond did not perturb the oligomerization state, nor did it affect the overall structure of β_2GPI, which remained elongated in solution. Since β_2GPI is believed to adopt "closed" and "open" forms (1), this information helps us to rule out a potential link between looping of the molecule and integrity of the disulfide bonds. Whether other mechanisms controlling circularization of β_2GPI exist, such as surface-induced oligomerization or reshuffling of disulfide bonds mediated by thiol-isomerases, remains a possibility. Thus far, however, we have no evidence that monomeric β_2GPI made recombinantly in mammalian cells or purified from plasma using the perchloric acid method can adopt a circular form in solution, as proposed by other research groups (12, 13).

An additional finding made possible by our reagents was the discovery that two disulfide bonds play very distinct structural roles in the context of protein folding. While absence of C32-C60 led to profound conformational changes in DI, which ultimately facilitated protein unfolding (Fig. 3), loss of C288-C326 imparted structural alterations that were well tolerated by the protein fold, with no measurable effects on the thermodynamic stability of β_2GPI. Based on this evidence, and according to the classification recently proposed by Chiu el al. (19), we conclude that the disulfide bond C32-C60 plays a "structural" role, whereas the disulfide bond C288-C326 is "allosteric." Given that the topology of the disulfide bond C32-C60 is conserved among CCP domains (6, 8–10), our results may also be relevant to other complement factors, such as complement factor H, which, similar to β_2GPI, acts at the interface of coagulation and complement cascades and whose detrimental function is linked to many human diseases, including APS (55).

Beyond the new structural insights, an important aspect of this study is that it provides an improved understanding of the role of the different reduced forms of β_2GPI in APS. In the context of aPL recognition, our biochemical data indicates that it is the disulfide bond C288-C326, and not C32-C60, that most heavily regulates protein's function. This is because the integrity of C288-C326 controls binding of β_2GPI to the plasma membranes (Fig. 4), and in turn, binding to the membranes is necessary for complex formation. Indeed, even though pathogenic antibodies in APS patients target DI of β_2GPI, loss of binding affinity due to the absence of the disulfide bond C32-C60 (Fig. 5) is not enough to prevent complex formation. Importantly, this scenario is consistent with a model of anti-β_2GPI/β_2GPI recognition originally proposed in the 1990s by several groups (see Table 2 of Giles *et al.* (56)) and recently extended by us (10), envisioning that the preferential binding of anti-DI antibodies to phospholipid-bound-β_2GPI arises from the ability of the preexisting elongated form to accumulate on the membranes. It also helps explain why increased levels of oxidative stress, which are believed to favor the oxidation the disulfide bond C288-C326 in circulating β_2GPI, may worsen disease in APS patients (20, 25). Interestingly, hydroxychloroquine (HQ) prevents formation of immune complexes by interfering with binding of β_2GPI to anionic phospholipids (57). Whether rupture of the disulfide bond C288-C326 contributes to the protective effects seen with HQ remains unknown.

Although less important for aPL recognition, the data obtained for the mutant β_2GPI C32S/C60S also merits attention, especially in the context of aPL generation. Since a relationship exists between misfolding of β_2GPI and autoantibody production (58), we speculate that reduction of the disulfide bond C32-C60 may facilitate the generation of aPL by favoring protein unfolding. Future studies facilitated by these reagents may help clarify whether APS belongs to the growing realm of protein folding diseases.

Experimental procedures

Protein expression, purification, and reagents

Human β_2GPI wild-type (residues 1–326, referred in this work as to oxβ_2GPI) modified to include an epitope for the HPC4 antibody at the N-terminal was cloned into a pDEST40 expression vector using the Gateway cloning technology (Life Technologies). The mutations C32S, C60S, C288S, C326S were generated using the Quickchange Lighting kit (Agilent) and appropriate primers (Integrated DNA Technologies). After sequencing, the recombinant proteins were expressed in ExpiHEK293 cells (Thermo Fisher Scientific) and purified by affinity chromatography, as described previously (10). The purity of each protein was verified by 4–12% SDS-PAGE (NuPAGE, Invitrogen) in the absence and presence of 2-Mercaptoethanol as a reducing agent. Proteins were aliquoted and stored at −80 °C until used. The proprietary monoclonal antibody MBB2 (patent number US2016/0152696A1) was produced and validated as described before (40). Protein concentrations were determined by reading at 280 nm with molar extinction coefficients adjusted according to the amino acid sequence. A value of 49,735 M^{-1} cm^{-1} was used for oxβ_2GPI, whereas values of 49,610 M^{-1} cm^{-1} were used for β_2GPI C32S/C60S and β_2GPI C288S/C326S. 1-palmitoyl-2-oleoyl-glycero-3-phosphocholine (POPC), 1-palmitoyl-2-oleoyl-sn-glycero-3-phospho-L-serine (POPS), and bovine heart cardiolipin sodium salt (CL) were from Avanti. All other chemicals were purchased from Sigma-Aldrich.

Deglycosylation experiments

oxβ_2GPI and variants (80 μl, 0.5 mg/ml) were mixed with 8 μl of deglycosylation buffer II (New England Biolabs) and incubated at 75 °C for 15 min to ensure denaturation of the protein samples. After 5 min at room temperature (20–22 °C), the solution was mixed with 5 μl of enzyme. The reaction was left for 3 h at 37 °C before quenching with 5× SDS-containing loading buffer (30 μl). Samples (40 μl/sample ∼10 μg) at t = 0 and t = 3 h were analyzed side by side on a 4–12%

SDS-PAGE (NuPAGE, Invitrogen). The gel was stained with SimplyBlue SafeStain following the manufacturers' protocols.

Fluorescent labeling

oxβ_2GPI and variants (50 μl, 5 μM) in Tris 20 mM, 145 mM NaCl, pH 7.4 were reacted with AlexaFluor 647-C2-maleimide (40 μM) (Thermo Fisher Scientific) in the absence or presence of TCEP (5 mM) for 2 h at room temperature (20–22 °C) in the dark. After 2 h, reactions were quenched with 50 mM DTT in SDS-containing loading buffer and run on a 4–12% SDS-PAGE (NuPAGE, Invitrogen). The gel was imaged on a Typhoon Gel and Blot Imaging Systems (Cytiva).

Size exclusion and heparin chromatography analyses

Immunopurified proteins were concentrated to 2 mg/ml by ultrafiltration using a MWCO of 10 kDa. After centrifugation (10,000*g* for 2 min), 100 μl (200 μg) of solution was loaded into a Superdex 200 HR 5/10 (Cytiva) at a flow rate of 0.5 ml/min that was equilibrated with Tris 20 mM, 145 mM NaCl at pH 7.4. Fifty microliters (100 μg) of the same 2 mg/ml solution was mixed with 150 μl of MilliQ water and loaded onto a HiTrap Heparin HP (1 ml). The column was eluted with a linear gradient of NaCl (50–500 mM in 15 min) at a flow rate of 0.8 ml/min. Absorbance was monitored at 280 nm using an ÄKTApurifier system (Cytiva).

Small-angle X-ray scattering (SAXS) measurements

SAXS data were collected at beamline 12-ID-B of the Advanced Photon Source at Argonne National Laboratory at concentration of 4 mg/ml in the absence and presence of glycerol and analyzed using the software ATSAS (59). Briefly, data sets of each protein sample and corresponding buffer were loaded into PRIMUS to obtain a baseline subtracted data set (*.dat). Baseline subtracted data sets were then analyzed using existing built-in applications, specifically radius of gyration (R_g) and pair distribution functions. The range used to calculate R_g was determined automatically by the software and carefully inspected to ensure linearity. The low-resolution envelopes were produced using DAMMIF (q up to 0.3 $Å^{-1}$) by directly fitting the reciprocal space-scattering profile. Twenty models were generated for every calculation and then aligned and averaged using DAMAVER. Output files were replotted in Datagraph and Pymol for visualization.

Fluorescence spectroscopy

Proteins were solubilized in 20 mM Tris pH 7.4, 145 mM NaCl (TBS) at a concentration of 200 nM. Tween 20 was added at a concentration of 0.015% (v/v) to minimize protein adsorption to the quartz cuvette. Since a small but significant signal variation of the fluorescent signal (10–15%) was detected over time even after addition of Tween 20, probably due to protein absorption to the quartz cuvette, all fluorescence spectra were collected exactly after 1 min from transferring the protein solutions into the quartz cuvette. For the chemical denaturation experiments, protein samples were prepared by mixing TBS-Tween buffer with a stock solution of 7.6 M Gnd-HCl prepared in 20 mM Tris pH 7.4, 145 mM NaCl into 1.5 ml plastic tubes to a final volume of 900 μl, followed by the addition 100 μl of 4 μM protein solution in TBS-T. Samples were incubated for at least 1 h at room temperature to allow the system to reach equilibrium. This was verified by incubating some protein samples overnight. Fluorescence spectra were recorded on a FluoroMax instrument equipped with water bath for temperature control. Protein samples were excited at 280 nm and the fluorescence intensity was recorded between 295 and 450 nm, using 5/10 nm as excitation and emission slits, respectively. The intensity at 350 nm corrected for baseline was then graphed as a function of denaturant concentration and fit to Equation 25 in ref. (60). Data reported in the manuscript represents the average of two independent experiments.

Surface plasmon resonance (SPR) experiments

Liposomes composed of 100% POPC, 80:20% (molar ratio) POPC:CL and 80:20% (molar ratio) POPC:POPS were prepared by extrusion using 100 nm polycarbonate membranes (Avanti) in TBS at a final concentration of 1 mM. They were kept at 4 °C and used within 7 days. Binding affinities for liposomes were measured using an L1 sensor chip in which liposomes were immobilized at 1600 ± 50 RU, as done before (10, 42). Titrations were performed by injecting increasing concentrations (0–5 μM) of β_2GPI and variants in running buffer (20 mM Tris pH 7.4, 150 mM NaCl, 0.1% w/w BSA) at a flow rate of 25 μl/min at 25 °C. Binding affinities for MBB2 were measured using CM7 sensor chip in which MBB2 was immobilized at 6000 RU using NHS/EDC chemistry. Titrations were performed by injecting increasing concentrations (0–20 μM) of β_2GPI and variants in running buffer (20 mM Tris pH 7.4, 145 mM NaCl, 0.01% w/w Tween20) at a flow rate of 25 μl/min at 25 °C. All experiments were carried out using on a BIAcore-S200 instrument (GE-Healthcare). The dissociation constants (K_d) were obtained as a fitting parameter by plotting the value of the response units (RU) at the steady state for each concentration using Origin Pro 2015. Data reported in the manuscript represents the average of three independent experiments.

ELISA assays

One-hundred microliter of a 10 μg/ml of oxβ_2GPI and variants solubilized in 0.1 M sodium bicarbonate pH 9.6 were added to a Nunc MAXISORP plate and incubated overnight at 4 °C. After washing three times with 200 μl/well of 20 mM Tris pH 7.4, 145 mM NaCl, 5 mM $CaCl_2$, Tween 20 0.02% (TBS-T), wells were blocked with 200 μl of 20 mM Tris pH 7.4, 145 mM NaCl, 5 mM $CaCl_2$, 1% BSA (TBS-B) for 60 min at room temperature. One-hundred microliters of plasma (1:60 v/v dilution) or MBB2 prepared in TBS-B was next added to each well and incubated for 60 min at room temperature. Plates were then washed three times TBS-T and then 100 μl of 1:10,000 dilution of alkaline phosphatase conjugated anti-human IgG (γ-chain specific) antibody (Sigma Aldrich) was added for 60 min at room temperature. Plates were washed

three times with TBS-T and then incubated with 100 µl of 3,3′,5,5′-tetramethylbenzidine (TMB) liquid substrate (Sigma Aldrich). After 30 min, the colorimetric reaction was quenched with 100 µl of TMB-stop solution. The optical density at 405 nm was recorded using a SPARK microplate reader (TECAN). Statistical analysis between the groups was performed using ANOVA in Prism 9.0.

Data availability

All data are contained in the manuscript. Deidentified plasma samples were provided by Prof Vittorio Pengo.

Acknowledgments—We are thankful to Dr Heyduk for granting access to the fluorimeter and for helpful discussions. This research used resources of the Advanced Photon Source, a U.S. Department of Energy (DOE) Office of Science User Facility, operated for the DOE Office of Science by Argonne National Laboratory under Contract No. DE-AC02-06CH11357.

Author contributions—S. K., M. C., and N. P. data curation; S. K., M. C., X. Z., and N. P. formal analysis; S. K., M. C., X. Z., and N. P. validation; S. K., M. C., W. P., X. Z., and N. P. investigation; S. K., M. C., W. P., X. Z., and N. P. methodology; S. K., M. C., X. Z., P. M., F. T., and N. P. writing–review and editing; P. M., F. T., and N. P. resources; N. P. conceptualization; N. P. supervision; N. P. funding acquisition; N. P. visualization; N. P. writing–original draft; N. P. project administration.

Funding and additional information—This work was supported in part by a grant R01 HL150146 (N. P.) from the National Heart, Lung, and Blood Institute.

Conflict of interest—The authors declare that they have no conflicts of interest with the contents of this article.

Abbreviations—The abbreviations used are: aCL, anticardiolipin; aPL, antiphospholipid; APS, antiphospholipid syndrome; β_2GPI, β_2-glycoprotein I; CCP, complement control protein; GpIbα, glycoprotein Ib alpha; LA, lupus anticoagulant; LUV, large unilamellar vesicle; MPB, 3-(N-maleimido-propionyl) biocytin; POPC:CL, phosphatidylcholine: cardiolipin; POPC:POPS, phosphatidylcholine: phosphatidylserine; SAXS, small-angle X-ray scattering; SEC, size-exclusion chromatography; SPR, surface plasmon resonance; TCEP, tris(2-carboxyethyl)phosphine hydrochloride; vWF, von Willebrand Factor.

References

1. de Groot, P. G., and Meijers, J. C. (2011) beta(2) -Glycoprotein I: evolution, structure and function. *J. Thromb. Haemost.* **9**, 1275–1284
2. Pozzi, N., Acquasaliente, L., Frasson, R., Cristiani, A., Moro, S., Banzato, A., Pengo, V., Scaglione, G. L., Arcovito, A., De Cristofaro, R., and De Filippis, V. (2013) beta2 -Glycoprotein I binds to thrombin and selectively inhibits the enzyme procoagulant functions. *J. Thromb. Haemost.* **11**, 1093–1102
3. Agar, C., de Groot, P. G., Morgelin, M., Monk, S. D., van Os, G., Levels, J. H., de Laat, B., Urbanus, R. T., Herwald, H., van der Poll, T., and Meijers, J. C. (2011) beta(2)-glycoprotein I: a novel component of innate immunity. *Blood* **117**, 6939–6947
4. Durigutto, P., Macor, P., Pozzi, N., Agostinis, C., Bossi, F., Meroni, P. L., Grossi, C., Borghi, M. O., Planer, W., Garred, P., and Tedesco, F. (2020) Complement activation and thrombin generation by MBL bound to beta2-glycoprotein I. *J. Immunol.* **205**, 1385–1392
5. Forneris, F., Wu, J., Xue, X., Ricklin, D., Lin, Z., Sfyroera, G., Tzekou, A., Volokhina, E., Granneman, J. C., Hauhart, R., Bertram, P., Liszewski, M. K., Atkinson, J. P., Lambris, J. D., and Gros, P. (2016) Regulators of complement activity mediate inhibitory mechanisms through a common C3b-binding mode. *EMBO J.* **35**, 1133–1149
6. Soares, D. C., and Barlow, P. N. (2005) *Structural Biology of the Complement System*, 1st Ed., Taylor & Francis, New York, NY
7. Hunt, J., and Krilis, S. (1994) The fifth domain of beta 2-glycoprotein I contains a phospholipid binding site (Cys281-Cys288) and a region recognized by anticardiolipin antibodies. *J. Immunol.* **152**, 653–659
8. Bouma, B., de Groot, P. G., van den Elsen, J. M., Ravelli, R. B., Schouten, A., Simmelink, M. J., Derksen, R. H., Kroon, J., and Gros, P. (1999) Adhesion mechanism of human beta(2)-glycoprotein I to phospholipids based on its crystal structure. *EMBO J.* **18**, 5166–5174
9. Schwarzenbacher, R., Zeth, K., Diederichs, K., Gries, A., Kostner, G. M., Laggner, P., and Prassl, R. (1999) Crystal structure of human beta2-glycoprotein I: Implications for phospholipid binding and the antiphospholipid syndrome. *EMBO J.* **18**, 6228–6239
10. Ruben, E., Planer, W., Chinnaraj, M., Chen, Z., Zuo, X., Pengo, V., De Filippis, V., Alluri, R. K., McCrae, K. R., Macor, P., Tedesco, F., and Pozzi, N. (2020) The J-elongated conformation of beta2-glycoprotein I predominates in solution: Implications for our understanding of antiphospholipid syndrome. *J. Biol. Chem.* **295**, 10794–10806
11. Baerenfaenger, M., and Meyer, B. (2019) Simultaneous characterization of SNPs and N-glycans from multiple glycosylation sites of intact beta-2-glycoprotein-1 (B2GP1) by ESI-qTOF-MS. *Biochim. Biophys. Acta Proteins Proteom.* **1867**, 556–564
12. Agar, C., van Os, G. M., Morgelin, M., Sprenger, R. R., Marquart, J. A., Urbanus, R. T., Derksen, R. H., Meijers, J. C., and de Groot, P. G. (2010) Beta2-glycoprotein I can exist in 2 conformations: Implications for our understanding of the antiphospholipid syndrome. *Blood* **116**, 1336–1343
13. Buchholz, I., McDonnell, T., Nestler, P., Tharad, S., Kulke, M., Radziszewska, A., Ripoll, V. M., Schmidt, F., Hammer, E., Toca-Herrera, J. L., Rahman, A., and Delcea, M. (2021) Specific domain V reduction of beta-2-glycoprotein I induces protein flexibility and alters pathogenic antibody binding. *Sci. Rep.* **11**, 4542
14. Hammel, M., Kriechbaum, M., Gries, A., Kostner, G. M., Laggner, P., and Prassl, R. (2002) Solution structure of human and bovine beta(2)-glycoprotein I revealed by small-angle X-ray scattering. *J. Mol. Biol.* **321**, 85–97
15. Ioannou, Y., Zhang, J. Y., Qi, M., Gao, L., Qi, J. C., Yu, D. M., Lau, H., Sturgess, A. D., Vlachoyiannopoulos, P. G., Moutsopoulos, H. M., Rahman, A., Pericleous, C., Atsumi, T., Koike, T., Heritier, S., *et al.* (2011) Novel assays of thrombogenic pathogenicity in the antiphospholipid syndrome based on the detection of molecular oxidative modification of the major autoantigen beta2-glycoprotein I. *Arthritis Rheum.* **63**, 2774–2782
16. Ioannou, Y., Zhang, J. Y., Passam, F. H., Rahgozar, S., Qi, J. C., Giannakopoulos, B., Qi, M., Yu, P., Yu, D. M., Hogg, P. J., and Krilis, S. A. (2010) Naturally occurring free thiols within beta 2-glycoprotein I *in vivo*: Nitrosylation, redox modification by endothelial cells, and regulation of oxidative stress-induced cell injury. *Blood* **116**, 1961–1970
17. Passam, F. H., Rahgozar, S., Qi, M., Raftery, M. J., Wong, J. W., Tanaka, K., Ioannou, Y., Zhang, J. Y., Gemmell, R., Qi, J. C., Giannakopoulos, B., Hughes, W. E., Hogg, P. J., and Krilis, S. A. (2010) Beta 2 glycoprotein I is a substrate of thiol oxidoreductases. *Blood* **116**, 1995–1997
18. Passam, F. H., Rahgozar, S., Qi, M., Raftery, M. J., Wong, J. W., Tanaka, K., Ioannou, Y., Zhang, J. Y., Gemmell, R., Qi, J. C., Giannakopoulos, B., Hughes, W. E., Hogg, P. J., and Krilis, S. A. (2010) Redox control of beta2-glycoprotein I-von Willebrand factor interaction by thioredoxin-1. *J. Thromb. Haemost.* **8**, 1754–1762
19. Chiu, J., and Hogg, P. J. (2019) Allosteric disulfides: Sophisticated molecular structures enabling flexible protein regulation. *J. Biol. Chem.* **294**, 2949–2960
20. Giannakopoulos, B., and Krilis, S. A. (2013) The pathogenesis of the antiphospholipid syndrome. *N. Engl. J. Med.* **368**, 1033–1044

21. Passam, F. H., Giannakopoulos, B., Mirarabshahi, P., and Krilis, S. A. (2011) Molecular pathophysiology of the antiphospholipid syndrome: The role of oxidative post-translational modification of beta 2 glycoprotein I. *J. Thromb. Haemost.* **9 Suppl 1**, 275–282
22. Weaver, J. C., Ullah, I., Qi, M., Giannakopoulos, B., Rye, K. A., Kockx, M., Kritharides, L., and Krilis, S. A. (2020) Free thiol beta2-GPI (beta-2-Glycoprotein-I) provides a link between inflammation and oxidative stress in atherosclerotic coronary artery disease. *Arterioscler Thromb. Vasc. Biol.* **40**, 2794–2804
23. Hulstein, J. J., Lenting, P. J., de Laat, B., Derksen, R. H., Fijnheer, R., and de Groot, P. G. (2007) beta2-Glycoprotein I inhibits von Willebrand factor dependent platelet adhesion and aggregation. *Blood* **110**, 1483–1491
24. Zhang, J. Y., Ma, J., Yu, P., Tang, G. J., Li, C. J., Yu, D. M., and Zhang, Q. M. (2017) Reduced beta 2 glycoprotein I prevents high glucose-induced cell death in HUVECs through miR-21/PTEN. *Am. J. Transl Res.* **9**, 3935–3949
25. Raimondo, M. G., Pericleous, C., Radziszewska, A., Borghi, M. O., Pierangeli, S., Meroni, P. L., Giles, I., Rahman, A., and Ioannou, Y. (2017) Oxidation of beta2-glycoprotein I associates with IgG antibodies to domain I in patients with antiphospholipid syndrome. *PLoS One* **12**, e0186513
26. Zhou, S., Lu, M., Zhao, J., Liu, S., Li, X., Zhang, R., Liu, H., and Yu, P. (2017) The purification of reduced beta2-glycoprotein I showed its native activity *in vitro*. *Lipids Health Dis.* **16**, 173
27. Chinnaraj, M., Barrios, D. A., Frieden, C., Heyduk, T., Flaumenhaft, R., and Pozzi, N. (2021) Bioorthogonal chemistry enables single-molecule FRET measurements of catalytically active protein disulfide isomerase. *Chembiochem* **22**, 134–138
28. Pace, C. N. (1990) Measuring and increasing protein stability. *Trends Biotechnol.* **8**, 93–98
29. Pozzi, N., Banzato, A., Bettin, S., Bison, E., Pengo, V., and De Filippis, V. (2010) Chemical synthesis and characterization of wild-type and biotinylated N-terminal domain 1-64 of beta2-glycoprotein I. *Protein Sci.* **19**, 1065–1078
30. Chen, Y., and Barkley, M. D. (1998) Toward understanding tryptophan fluorescence in proteins. *Biochemistry* **37**, 9976–9982
31. Galli, M., Comfurius, P., Maassen, C., Hemker, H. C., de Baets, M. H., van Breda-Vriesman, P. J., Barbui, T., Zwaal, R. F., and Bevers, E. M. (1990) Anticardiolipin antibodies (ACA) directed not to cardiolipin but to a plasma protein cofactor. *Lancet* **335**, 1544–1547
32. Subang, R., Levine, J. S., Janoff, A. S., Davidson, S. M., Taraschi, T. F., Koike, T., Minchey, S. R., Whiteside, M., Tannenbaum, M., and Rauch, J. (2000) Phospholipid-bound beta 2-glycoprotein I induces the production of anti-phospholipid antibodies. *J. Autoimmun.* **15**, 21–32
33. Guerin, J., Sheng, Y., Reddel, S., Iverson, G. M., Chapman, M. G., and Krilis, S. A. (2002) Heparin inhibits the binding of beta 2-glycoprotein I to phospholipids and promotes the plasmin-mediated inactivation of this blood protein. Elucidation of the consequences of the two biological events in patients with the anti-phospholipid syndrome. *J. Biol. Chem.* **277**, 2644–2649
34. Shaw, A. W., Pureza, V. S., Sligar, S. G., and Morrissey, J. H. (2007) The local phospholipid environment modulates the activation of blood clotting. *J. Biol. Chem.* **282**, 6556–6563
35. Meroni, P. L., Borghi, M. O., Raschi, E., and Tedesco, F. (2011) Pathogenesis of antiphospholipid syndrome: Understanding the antibodies. *Nat. Rev. Rheumatol.* **7**, 330–339
36. de Groot, P. G., and Urbanus, R. T. (2012) The significance of autoantibodies against beta2-glycoprotein I. *Blood* **120**, 266–274
37. de Laat, B., Derksen, R. H., van Lummel, M., Pennings, M. T., and de Groot, P. G. (2006) Pathogenic anti-beta2-glycoprotein I antibodies recognize domain I of beta2-glycoprotein I only after a conformational change. *Blood* **107**, 1916–1924
38. Banzato, A., Pozzi, N., Frasson, R., De Filippis, V., Ruffatti, A., Bison, E., Padayattil, S. J., Denas, G., and Pengo, V. (2011) Antibodies to Domain I of beta(2)Glycoprotein I are in close relation to patients risk categories in Antiphospholipid Syndrome (APS). *Thromb. Res.* **128**, 583–586
39. de Laat, B., Derksen, R. H., Urbanus, R. T., and de Groot, P. G. (2005) IgG antibodies that recognize epitope Gly40-Arg43 in domain I of beta 2-glycoprotein I cause LAC, and their presence correlates strongly with thrombosis. *Blood* **105**, 1540–1545
40. Agostinis, C., Durigutto, P., Sblattero, D., Borghi, M. O., Grossi, C., Guida, F., Bulla, R., Macor, P., Pregnolato, F., Meroni, P. L., and Tedesco, F. (2014) A non-complement-fixing antibody to beta2 glycoprotein I as a novel therapy for antiphospholipid syndrome. *Blood* **123**, 3478–3487
41. Agostinis, C., Biffi, S., Garrovo, C., Durigutto, P., Lorenzon, A., Bek, A., Bulla, R., Grossi, C., Borghi, M. O., Meroni, P., and Tedesco, F. (2011) *In vivo* distribution of beta2 glycoprotein I under various pathophysiologic conditions. *Blood* **118**, 4231–4238
42. Chinnaraj, M., Planer, W., Pengo, V., and Pozzi, N. (2019) Discovery and characterization of 2 novel subpopulations of aPS/PT antibodies in patients at high risk of thrombosis. *Blood Adv.* **3**, 1738–1749
43. Proulle, V., Furie, R. A., Merrill-Skoloff, G., Furie, B. C., and Furie, B. (2014) Platelets are required for enhanced activation of the endothelium and fibrinogen in a mouse thrombosis model of APS. *Blood* **124**, 611–622
44. Silverberg, M., and Diehl, S. V. (1987) The autoactivation of factor XII (Hageman factor) induced by low-Mr heparin and dextran sulphate. The effect of the Mr of the activating polyanion. *Biochem. J.* **248**, 715–720
45. Pixley, R. A., Cassello, A., De La Cadena, R. A., Kaufman, N., and Colman, R. W. (1991) Effect of heparin on the activation of factor XII and the contact system in plasma. *Thromb. Haemost.* **66**, 540–547
46. Morrissey, J. H., Choi, S. H., and Smith, S. A. (2012) Polyphosphate: An ancient molecule that links platelets, coagulation, and inflammation. *Blood* **119**, 5972–5979
47. Schousboe, I. (1985) Beta 2-Glycoprotein I: a plasma inhibitor of the contact activation of the intrinsic blood coagulation pathway. *Blood* **66**, 1086–1091
48. Iverson, G. M., Victoria, E. J., and Marquis, D. M. (1998) Anti-beta2 glycoprotein I (beta2GPI) autoantibodies recognize an epitope on the first domain of beta2GPI. *Proc. Natl. Acad. Sci. U. S. A.* **95**, 15542–15546
49. Butera, D., and Hogg, P. J. (2020) Fibrinogen function achieved through multiple covalent states. *Nat. Commun.* **11**, 5468
50. Butera, D., Passam, F., Ju, L., Cook, K. M., Woon, H., Aponte-Santamaria, C., Gardiner, E., Davis, A. K., Murphy, D. A., Bronowska, A., Luken, B. M., Baldauf, C., Jackson, S., Andrews, R., Grater, F., *et al.* (2018) Autoregulation of von Willebrand factor function by a disulfide bond switch. *Sci. Adv.* **4**, eaaq1477
51. Muller-Calleja, N., Ritter, S., Hollerbach, A., Falter, T., Lackner, K. J., and Ruf, W. (2018) Complement C5 but not C3 is expendable for tissue factor activation by cofactor-independent antiphospholipid antibodies. *Blood Adv.* **2**, 979–986
52. Essex, D. W., and Li, M. (2003) Redox control of platelet aggregation. *Biochemistry* **42**, 129–136
53. Li, J., Kim, K., Jeong, S. Y., Chiu, J., Xiong, B., Petukhov, P. A., Dai, X., Li, X., Andrews, R. K., Du, X., Hogg, P. J., and Cho, J. (2019) Platelet protein disulfide isomerase promotes glycoprotein Ibalpha-mediated platelet-neutrophil interactions under thromboinflammatory conditions. *Circulation* **139**, 1300–1319
54. Stopa, J. D., Neuberg, D., Puligandla, M., Furie, B., Flaumenhaft, R., and Zwicker, J. I. (2017) Protein disulfide isomerase inhibition blocks thrombin generation in humans by interfering with platelet factor V activation. *JCI Insight* **2**, e89373
55. Chaturvedi, S., Braunstein, E. M., Yuan, X., Yu, J., Alexander, A., Chen, H., Gavriilaki, E., Alluri, R., Streiff, M. B., Petri, M., Crowther, M. A., McCrae, K. R., and Brodsky, R. A. (2020) Complement activity and complement regulatory gene mutations are associated with thrombosis in APS and CAPS. *Blood* **135**, 239–251
56. Giles, I. P., Isenberg, D. A., Latchman, D. S., and Rahman, A. (2003) How do antiphospholipid antibodies bind beta2-glycoprotein I? *Arthritis Rheum.* **48**, 2111–2121
57. Rand, J. H., Wu, X. X., Quinn, A. S., Chen, P. P., Hathcock, J. J., and Taatjes, D. J. (2008) Hydroxychloroquine directly reduces the binding of

antiphospholipid antibody-beta2-glycoprotein I complexes to phospholipid bilayers. *Blood* **112**, 1687–1695

58. de Laat, B., van Berkel, M., Urbanus, R. T., Siregar, B., de Groot, P. G., Gebbink, M. F., and Maas, C. (2011) Immune responses against domain I of beta(2)-glycoprotein I are driven by conformational changes: domain I of beta(2)-glycoprotein I harbors a cryptic immunogenic epitope. *Arthritis Rheum.* **63**, 3960–3968
59. Franke, D., Petoukhov, M. V., Konarev, P. V., Panjkovich, A., Tuukkanen, A., Mertens, H. D. T., Kikhney, A. G., Hajizadeh, N. R., Franklin, J. M., Jeffries, C. M., and Svergun, D. I. (2017) Atsas 2.8: A comprehensive data analysis suite for small-angle scattering from macromolecular solutions. *J. Appl. Crystallogr.* **50**, 1212–1225
60. Eftink, M. R. (1994) The use of fluorescence methods to monitor unfolding transitions in proteins. *Biophys. J.* **66**, 482–501